

3D geological and potential field modelling of the buried alkaline-carbonatite Tajno massif (East European Craton, NE Poland)

Zdzisław PETECKI^{1,*}, Olga ROSOWIECKA¹ and Leszek KRZEMIŃSKI¹

¹ Polish Geological Institute – National Research Institute, Rakowiecka 4, 00-975 Warszawa, Poland



Petecki, Z., Rosowiecka, O., Krzemiński, L., 2022. 3D geological and potential field modelling of the buried alkaline-carbonatite Tajno massif (East European Craton, NE Poland). *Geological Quarterly*, 66: 10, doi: 10.7306/gq.1642

Associate Editor: Jacek Szczepański

Geological and geophysical data are used to model the 3D geometry of the Tajno alkaline massif intruded during the Early Carboniferous in NE Poland. The massif consists mainly of pyroxenite, mafic intrusive and volcanic rocks, and carbonatites containing rare earth elements (REE) and other important mineral resources. The deep structure of the massif, and its thickness, shape and internal structure, has been poorly known making it impossible to properly search for useful mineral resources. In order to better constrain the distribution, geometries and relationships between the main rock types, a 3D geological model of the Tajno massif has been developed. The input data comprise a set of geological cross-sections built on an updated subsurface geological map, and borehole, magnetic and gravity data. 3D *Geomodeller* software was applied to integrate geological data into a coherent and geologically feasible model of the massif using geostatistical analysis. The magnetic and gravity data were used to constrain the 3D geological modelling results. The final 3D model is thus compatible with the geological data, as well as with geophysical data. The most important conclusions obtained from the modelling are as follows: (i) a higher proportion of nepheline syenites or tuffs and pyroclastic breccia in relation to pyroxenites; and, (ii) a smaller proportion of chimney breccia relative to chimney-hosted tuffs and volcanic breccia than proposed in previous geological interpretation. These results are important for further studies on the evolution of the Tajno massif and its associated carbonatites.

Key words: Tajno alkaline massif, NE Poland, 3D geological and geophysical modelling, *GeoModeller*.

INTRODUCTION

The alkaline-carbonatite plutonic-volcanic Tajno massif belongs to the magmatic structures formed during Paleozoic time in the western part of the East European Craton (EEC), in NE Poland (Krzemińska et al., 2017; Fig. 1). The massif intruded the Paleoproterozoic crystalline basement and is covered by 600 m of sedimentary overburden.

The Tajno massif was discovered as a result of drilling into remarkable positive magnetic and gravity anomalies in NE Poland (Cieśla and Kosobudzka, 1992). These investigations revealed the presence of alkaline ultramafic rocks within the crystalline basement (Kubicki, 1992). Being a potential site of REE ore deposits, the Tajno massif has been studied geophysically, petrologically and structurally (Cieśla and Kosobudzka, 1992; Kubicki, 1992; Ryka, 1992; Ryka et al., 1992; Wiszniewska et

al., 2020). Magnetic and gravity investigations have outlined the major structural features of the Tajno massif. Direct information on the nature and structure of the basement is limited to 12 unevenly distributed deep boreholes. Due to this sparse geological data it has not been possible to construct more than one reliable geological cross-section through the massif (Kubicki, 1992).

Despite the previous studies, the deep structure of the massif is still not well understood. Therefore, with existing geological data, it is difficult to propose a coherent model of the 3D geological architecture of the massif that would enable its exploration as regards potentially economic accumulations of REE mineralization.

Resolving the geometry and internal structure of the massif are key aims of geological and geophysical interpretation, and in this study we constrain the spatial structure of the Tajno massif by means of 3D geological modelling. The *GeoModeller* software package was used to create a realistic 3D geological model constrained by all available geological data. Analysis of the geophysical data took place in the process of creating an initial 3D geological model of the massif. Furthermore, 3D forward modelling of the gravity and magnetic fields was carried out to evaluate the reliability of this model, and to further refine the model geometry.

* Corresponding author, e-mail: zdzislaw.petecki@pgi.gov.pl

Received: August 6, 2021; accepted: March 20, 2022; first published online: April 21, 2022

GEOLOGICAL CONTEXT

The Tajno alkaline-carbonatite massif is one of the group of intrusive structures within the crystalline basement of the EEC in northeastern Poland. The massif, covering an area of 5 km², is buried beneath 600 m of Mesozoic and Cenozoic sedimentary rocks. It is located within a narrow alkaline magmatic belt in the Paleoproterozoic Mazowsze Domain, which trends E–W from SW Lithuania to NE Poland, along the southern rim of the Mesoproterozoic Mazury Complex (Fig. 1; Bogdanova et al., 2015; Krzemińska et al., 2017; Wiszniewska et al., 2020). In the Mazowsze Domain the most typical rocks are mafic to felsic metavolcanics and granitoids (Fig. 2A; Wiszniewska et al., 2020).

In addition to the Tajno massif, at least four other alkaline massifs: the Elk alkaline syenite massif, the Pisz gabbro-syenite intrusion, and the Mława and the Olsztynek syenite

intrusions were originally discovered by the Polish Geological Institute (PGI) using gravity, magnetic and drilling data (Fig. 1; Kubicki and Ryka, 1982; Krzemińska et al., 2017). Three intrusions (Pisz, Elk and Tajno) have been dated: U-Pb dating on zircons from Pisz, Elk and Tajno rocks gave ages 345.5 ± 5.1 Ma, 347.7 ± 7.9 Ma and 348 ± 15 Ma, respectively; and, a pyrrhotite from a Tajno carbonatite vein dated using the Re-Os method yielded an age of 348 Ma (Demaiffe et al., 2013).

Twelve boreholes have been drilled up to a maximum depth of 1800 m into rocks of the Tajno massif by the PGI (Fig. 2B). These boreholes revealed that the Tajno massif is a multi-phase volcano-plutonic intrusion penetrating metamorphic, orthogneissic basement. The boreholes located in the central part of the structure penetrated a palaeovolcanic vent filled with intrusive breccia and pyroclastic and volcanic rocks of the chimney breccia, cut by mafic dykes (Kubicki, 1992).

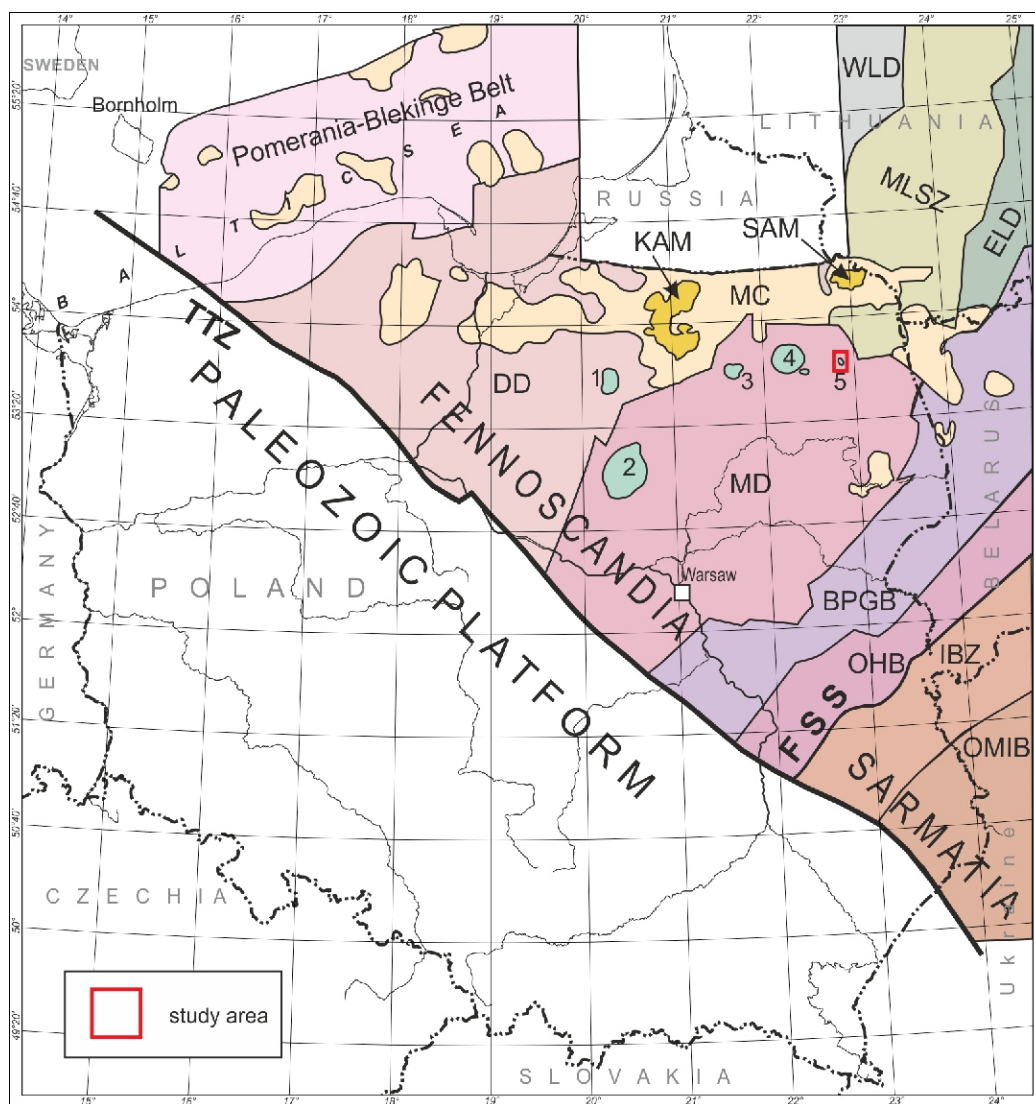


Fig. 1. Major crustal domains of crystalline basement in the Polish part of the East European Platform modified after Krzemińska et al. (2017)

Fault zones: TTZ – Teisseyre-Tornquist Zone, FSS – Fennoscandia-Sarmatia Suture; crustal domains: MC – Mazury Complex, MD – Mazowsze Domain, DD – Dobrzyń Domain, MLSZ – Mid-Lithuanian Suture Zone, WLD – West Lithuanian Domain, ELD – East Lithuanian Domain, BPGB – Belarus-Podlasie Granulite Belt, OHB – Okolowo-Holeszów Belt, IBZ – Ivano-Borisov Zone, OMIB – Osnitsk-Mikashevichi Igneous Belt; Mesoproterozoic massifs and intrusions: SAM – Suwałki Anorthosite Massif, KAM – Kętrzyn Anorthosite Massif; Paleozoic massifs and intrusions: 1 – Olsztynek, 2 – Mława, 3 – Pisz, 4 – Elk, 5 – Tajno

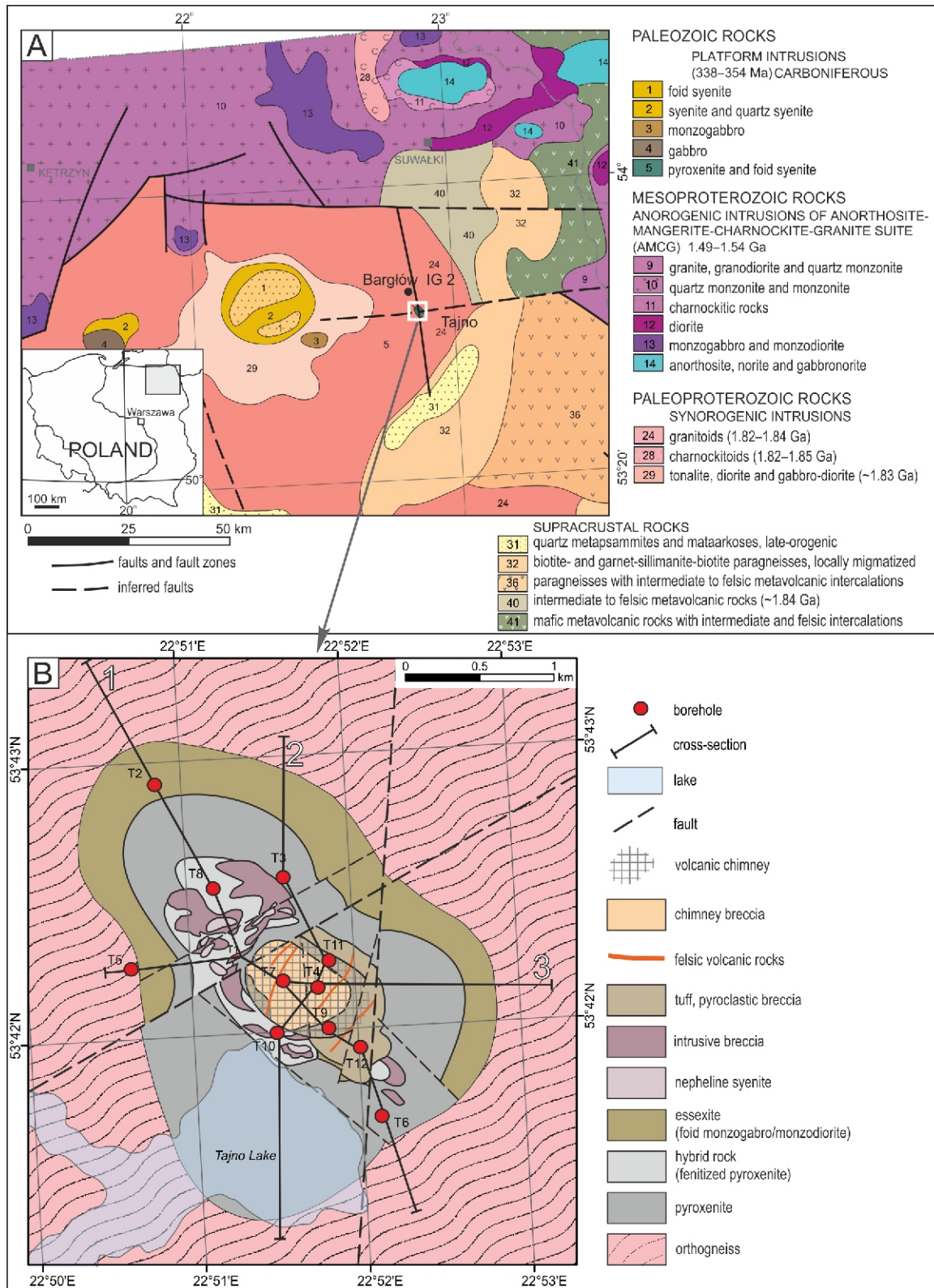


Fig. 2B – geological map of the crystalline basement of NE Poland (after Krzemińska et al., 2017) and location of the Tajno area (box); **B** – geological map of the Tajno massif area at the level of 500 m b.s.l. based on integrated geological and geophysical data interpreted in this paper

T1–T12: location of the Tajno IG 1 – Tajno IG 12 boreholes

The intrusion, consisting mainly of clinopyroxenites, hybrid rocks (fentitized pyroxenites), essexites, syenites and various volcanic rocks, is cut by carbonatite veins of variable thickness (up to 50 cm, though 95% up to 1 cm) with potentially economic accumulation of REEs (Krystkiewicz and Krzemiński, 1992; Kubicki, 1992; Ryka, 1992; Ryka et al., 1992). REE-bearing minerals (burbankite, parisite, synchysite and bastnaesite) which are highly enriched in such elements as Sr, Ba and LREE, are common in Tajno carbonatites (Ryka, 1992). These minerals are distributed very heterogeneously in the carbonatite veins and in the carbonatitic cement of the chimney breccia. Therefore, Kubicki (1992) estimated a REE₂O₃ content varying between 0.1 and 0.5%, whereas Ryka (1992) suggested values ranging from 0.2 to 1.3%.

MAGNETIC AND GRAVITY DATA

Potential field anomaly analysis is a useful tool for investigating the subsurface structure of the Tajno massif. Therefore, this study provides an interpretation of the available magnetic and gravity data to examine the spatial distribution of lithologies within the massif.

Detailed magnetic and gravity studies were carried out over the central part of the magnetic and gravity anomalies related to the Tajno massif, with grid density of 0.15 km and outside the central part on a regular 0.3 km grid basis (Cieśla and Kosobudzka, 1992). The southern edges of the anomalies are insufficiently documented due to the presence of Lake Tajno and adjoining swamps. However, magnetic measurements have been carried out on Lake Tajno (Cieśla and Kosobudzka, 1992).

The magnetic data from the Tajno area (Fig. 3A) is represented as a total magnetic intensity anomaly map. The total magnetic intensity anomaly was obtained by subtracting the magnitude of an appropriate DGRF (Definitive Geomagnetic Reference Field) 1982.5 regional field from the total field measurement (Petecki and Rosowiecka, 2017).

The gravity data is represented by a Bouguer anomaly map (Fig. 3B). The gravity measurements are tied to the international IGSN71 (International Gravity Standardization Net of 1971) gravity reference and reduced to simple Bouguer anomalies using the GRS 80 (Geodetic Reference System of 1980) formula for the theoretical gravity, and a reduction density of 2250 kg/m³ (Królikowski and Petecki, 1995).

Based on the available data, the Tajno massif appears as large positive, magnetic (1550 nT) and gravity (6.5 mGal) anomalies that are clearly marked in the low-amplitude regional magnetic and gravity patterns. They are both characterized by a nearly circular shape, bounded by high gradient zones, and show a good correlation between each other suggesting that both anomalies are caused by the same igneous body, with intense magnetic susceptibility and density contrasts between the intrusive rocks and their host basement. Petrographic data obtained from boreholes have clearly indicated the relationship between the geophysical anomalies and the alkaline ultramafic rocks (Kubicki, 1992; Wiszniewska et al., 2020). Large magnetic susceptibility and density contrasts between the alkaline rocks of the Tajno Massif and surrounding rocks of the basement have further been established by laboratory measurements of the physical properties of the rocks studied.

Geophysical investigations that included detailed ground magnetic and gravity data were used to constraint the 3D geological modelling of the Tajno massif. The available magnetic and gravity data have been processed for better visualization of structural features of the Tajno massif. Magnetic data processing included reduction to the pole (RTP) and analytical down-

ward continuation to a depth of 600 m. The RTP method transforms the observed magnetic anomalies into the anomalies that would have been measured if both the magnetization and ambient field were vertical to bring anomalies directly over their geological sources. Downward continuation transforms the potential field measured on one surface to the field that would be measured on another surface nearer to sources to enhance details of the source distribution (Blakely, 1995).

The resulting RTP map is shown in Figure 4A. Reduction to the pole, in comparison with the original total intensity magnetic map (Fig. 3A), results in a slightly northwards migration of the magnetic anomalies, due to the elimination of the inclination and declination of the magnetic field in this area. The positive magnetic anomaly maximum, formerly located over Lake Tajno (Fig. 3A), is now situated on the RTP map (Fig. 4A) near the Tajno IG 8 borehole.

Downward continuation of the RTP map to the crystalline basement top (600 m depth; Fig. 4B) greatly enhanced the pattern of anomaly maxima and minima and gradient zones, providing a more detailed outline of the Tajno massif. The gravity anomaly map (Fig. 3B) has been transformed using the band-pass Butterworth filter with wavelength cut-offs at 800 m and 2500 m. The petrophysical diversity of the Tajno massif is also visible in this gravity anomaly map (Fig. 4C).

Analysis of the transformed magnetic and gravity anomalies (Fig. 4B, C) suggests separation of anomaly patterns into two main domains, with characteristic amplitudes, i.e. a circular zone of magnetic and gravity lows, especially strongly manifested in the magnetic field, located in the central part of the massif, and a second domain of magnetic and gravity highs surrounding the central domain. The boreholes situated within the central domain (e.g., Tajno IG 4 borehole) penetrated the vent of a palaeovolcano filled with chimney breccia and pyroclastic materials (Kubicki, 1992; Wiszniewska et al., 2020). These rocks are characterized by weak magnetic properties and low densities (Cieśla and Kosobudzka, 1992). Rocks with strong magnetic properties and of high density are dominant in the second domain (Cieśla and Kosobudzka, 1992), especially in its western and northern parts (Tajno IG 8 borehole), and are related mainly to the presence of clinopyroxenites (Kubicki, 1992; Wiszniewska et al., 2020).

ROCK PROPERTY DATA

Information on the properties of rocks from the Tajno massif was analyzed using archival data from the National Geological Archive as an important part of the 3D geological modelling procedure. A relatively large number of density and magnetic property measurements are available to compute the gravity and magnetic response of the 3D geological model. The mean density and magnetic property measurements of the crystalline basement core rock samples from the boreholes are shown in Table 1, and the average density and magnetic property values for sedimentary formations and each major rock type are given in Table 2. However, the variability of physical properties within the rock types makes it difficult to reliably estimate the average density, magnetic susceptibility (MS), natural remanent magnetization (NRM) and direction of magnetization values of the main rock types. In addition, due to the wide compositional range, particular samples used for the measurements may not be representative. Therefore, the average (mean) physical property values for each major rock type are taken to be representative of the physical property variations, and are used as the initial estimates for gravity and magnetic forward modelling (Table 2).

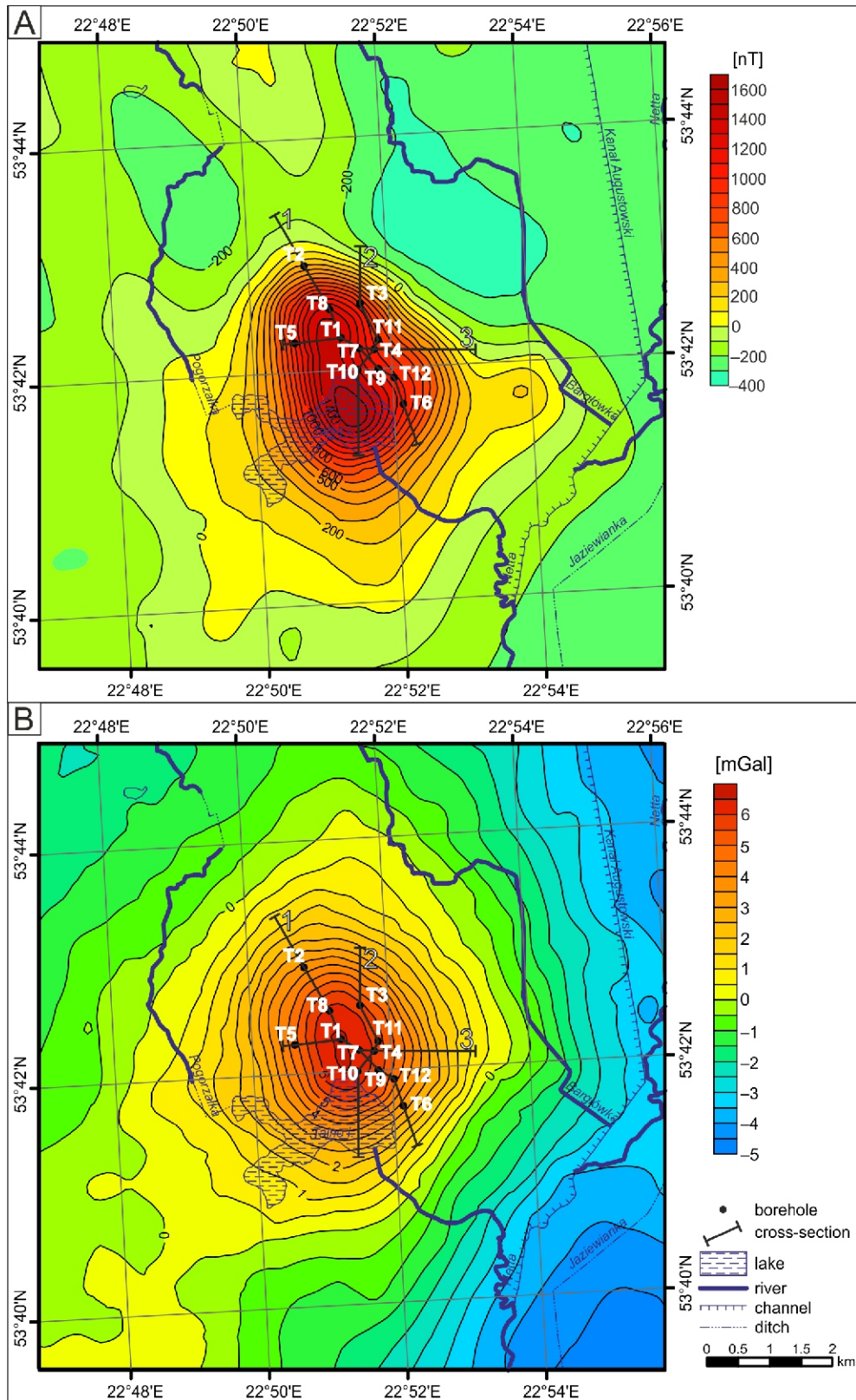


Fig. 3A – total intensity magnetic anomaly map; B – Bouguer gravity anomaly map

T1–T12 as in Figure 2

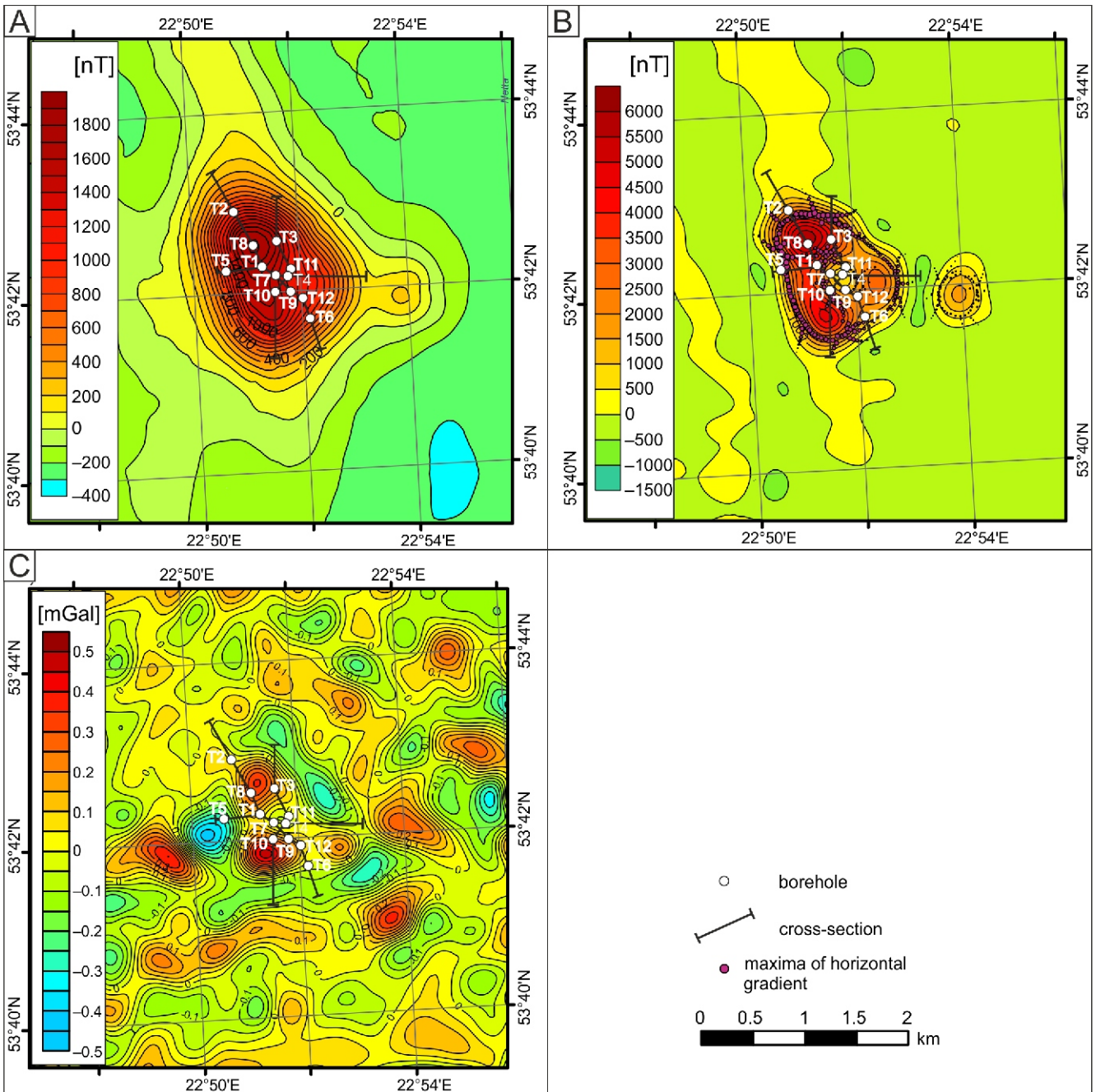


Fig. 4A – reduced-to-the-pole (RTP) total intensity magnetic anomaly map; **B** – reduced-to-the-pole, downward-continued to a depth of 600 m and low-pass filtered with a cut-off wavelength of 1000 m total intensity magnetic anomaly map with maxima of horizontal gradient (purple dots) superimposed; **C** – residual gravity anomaly map computed using band-pass Butterworth filter with wavelength cut-offs 800 m and 2500 m

T1 – T12 as in [Figure 2](#)

DENSITY DATA

The estimated mean densities from borehole data indicate that the Tajno intrusion has variable densities of 2770–3360 kg/m³ with high densities generally dominating ([Table 1](#)). The mean density of rocks directly bordering the Tajno massif, i.e. orthogneisses, has a moderate value of 2710 kg/m³, based on measurements from one borehole (Tajno IG 5), distinctly less than that of the massif rocks. This results in a high gravity anomaly related to the massif.

The densities of pyroxenites and fenitized pyroxenites that form the main part of the Tajno massif are high, 3010 and 3430 kg/m³, respectively ([Table 2](#)). High densities, with a mean value of 3030 kg/m³, are also related to essexite encountered in the Tajno IG 2 borehole, and intrusive breccia (2900 kg/m³). The density of crater facies rocks (chimney breccias, tuff and pyroclastic breccias) ranges from 2750 to 2850 kg/m³. The mean density of rocks derived from the Tajno IG 4 borehole which penetrated the crater of a palaeovolcano has an average value of 2770 kg/m³ ([Table 1](#)). The syenite rocks that were

Table 1

Average density and magnetic properties of crystalline basement rocks in the boreholes

Borehole	Density [kg/m ³]	Magnetic susceptibility [SI]	NRM intensity [A/m]	Koenigsberger coefficient	Inclination [°] n – samples
Tajno IG 1	2960	0.136596	4.99	1.03	N/A
Tajno IG 2	3030	0.204706	3.93	0.7	+77.5 (n=150) -77.7 (n=44)
Tajno IG 3	3250	0.208853	7.10	0.9	N/A
Tajno IG 4	2770	0.018975	1.10	0.44	+42 (n=75) -37 (n=26)
Tajno IG 5	2710	0.050642	0.88	0.4	N/A
Tajno IG 6	3360	0.267915	7.55	0.7	N/A
Tajno IG 8	3010	0.166504	17.03	2.41	+69 (n=55)
Tajno IG 9	N/A	0.084521	N/A	N/A	N/A
Tajno IG 10	N/A	0.086142	N/A	N/A	N/A
Tajno IG 11	N/A	0.037699	N/A	N/A	N/A
Tajno IG 12	2830	0.109327	0.9	0.3	+50 (n=64) -52 (n=16)

Table 2

Average density and magnetic properties of sedimentary successions and crystalline basement rock types

Geological formation	Density [kg/m ³]	Magnetic susceptibility [SI]	NRM intensity [A/m]	Koenigsberger coefficient	Inclination [°]
Cenozoic	1700	0	0	0	0
Cretaceous	1750	0	0	0	0
Jurassic	1780	0	0	0	0
Triassic	2150	0	0	0	0
Chimney breccia	2750	0.02	1.1	0.44	21.6
Felsic volcanic rocks	N/A	N/A	N/A	N/A	N/A
Melanephelinite	2990	0.15	1	0.2	50
Tuff, pyroclastic breccia	2850	0.125	0.9	0.1	40
Intrusive breccia	2900	0.14	15	2	69
Nepheline syenite	2660	0.06	2	0.87	69
Essexite (foid monzogabro /monzodiorite)	3030	0.20	3.93	0.7	42.3
Hybrid rock (fentized pyroxenite)	3170	0.20	16.6	2.3	69
Pyroxenite	3300	0.28	28	2.7	69
Orthogneiss	2710	0.05	0.88	0.4	30

drilled by the Tajno IG 8 borehole (Fig. 5) have the lowest average density of all rock types of the massif (2660 kg/m³; Table 2).

MAGNETIC PROPERTY DATA

The mean MS from boreholes drilled in the Tajno massif varies between 0.019 and 0.268 SI (Table 1). The lowest mean MS characterizes the crater-rock facies drilled by the Tajno IG 4 borehole while the rocks drilled by the boreholes situated outside the crater display distinctly higher MS. The mean MS of rocks bordering the Tajno massif has a value of 0.05 SI (Tajno IG 5 borehole). However, the MS of basement rocks from the

Tajno area shows considerable scatter. For example, MS was found to vary between 0.003 and 0.475 SI for rocks drilled by the Tajno IG 8 borehole (Fig. 5).

The MS of pyroxenites and hybrid rocks (fentized pyroxenites) are high on average, 0.28 and 0.20 SI, respectively (Table 2). These rocks are also characterized by high values of NRM (28 and 16.6 A/m), decidedly dominating their inductive magnetization (Cieśla and Kosobudzka, 1992). The NRM inclinations of are positive, with an average value of 69° as observed in the Tajno IG 8 borehole.

Essexite shows high MS (0.2 SI), the same as for intrusive breccia (0.14 SI). The chimney breccia is characterized by low

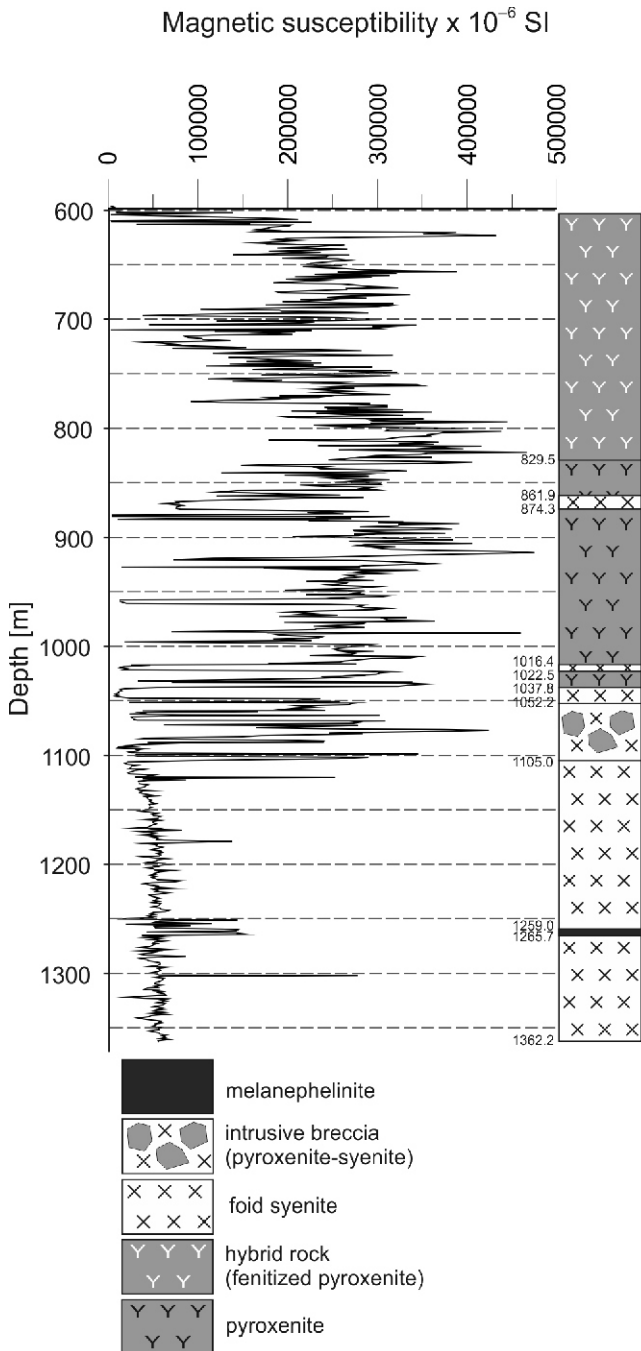


Fig. 5. Magnetic susceptibility in the Tajno IG 8 borehole

MS (0.02 SI) but tuff and pyroclastic breccia (0.125 SI) and melanephelinite (0.15 SI) have distinct magnetic properties.

The ratio of the intensity of NRM to induced magnetization, termed the Koenigsberger coefficient or Q , ranges from 0.3 to 2.41 (Table 1), and is commonly less than 1.0 in all but two of the boreholes. The low values of the Q ratio demonstrate that induced magnetization would either dominate or be comparable to that of the remanent magnetization. At all boreholes, the direction of the NRM inclination varies largely but is predominantly positive (80% of measurements show positive inclination).

In contrast, the measured NRM inclinations of samples from the Tajno IG 8 borehole are all positive with an average value of $+69^\circ$, similar to that of the present Earth magnetic field

(Table 1). Measurements on samples of pyroxenite and hybrid rock (fentitized pyroxenite) from this borehole (Fig. 5) indicate the presence of significant NRM dominating the total magnetization ($Q=2.41$).

IDEAL-BODY ANALYSIS OF THE GRAVITY DATA

The ideal-body inversion has been applied to the gravity profile over the Tajno massif using the program described by Huestis and Ander (1983), modified by Petecki (2019), to be capable of treating the 2.5 D interpretation approach. The objective of this method is to find the bounds on density contrast, depth, and minimum thickness of the causative body that can explain the gravity anomaly within a given misfit (Parker, 1974, 1975).

In order to obtain the best representation of the short wavelength nature of the Tajno gravity anomaly, a high-pass filter with a cut-off wavelength of 20 km was applied to the Bouguer anomaly (Fig. 6).

To constrain the smallest density contrast and minimum thickness of the Tajno massif, the ideal body inversion was performed on the 9 data sampled from the residual gravity anomaly map along profile A–A' (Fig. 6). A depth to anomalous body of 0.6 km was estimated from deep boreholes located over the anomaly. Therefore, the inverse calculation assumed that the ideal body top is confined below 0.6 km. The domain in which the ideal body is allowed to be located was divided into a series of 2.5D rectangular prisms whose horizontal and vertical dimensions along the profile were 0.1 km and 0.1 km, respectively, while their lateral extent was ± 1.5 km in the direction perpendicular to the profile. A misfit of 0.1 mGal was assumed for the gravity values used in the calculations.

The smallest maximum density contrasts are plotted against corresponding values of thickness of the Tajno anomalous body on the trade-off curve (Fig. 7). The smallest maximum density contrast is equal to 310 kg/m^3 , with a maximum allowable thickness of 2 km for the source body. In other words, models with the density contrast at or above 310 kg/m^3 fit the gravity data within the specified (0.1 mGal) misfit level.

On the other hand, Figure 7 shows the minimum thickness of the ideal body if the maximum density contrast of the source can be assumed as a result of drilling studies, or on the basis of geological information.

To find the largest reasonable density contrast it was assumed the rocks of the massif with a density of 3360 kg/m^3 (Tajno IG 6) are surrounded by orthogneisses (Tajno IG 5) with a density of 2710 kg/m^3 (Table 1). Taking these values into consideration the maximum density contrast will be 650 kg/m^3 . For this maximum density contrast the minimum thickness of ideal body is 0.5 km.

Assuming that a more realistic density for the source of the Tajno anomaly is the average density of massif rocks (3030 kg/m^3), the density contrast will be 320 kg/m^3 . This hypothetical density contrast is based on 2251 density measurements of massif rock samples. If the maximum possible density contrast is only 320 kg/m^3 , the source body can be no thinner than 1.48 km.

Summarizing, if the maximum density contrast is not greater than 320 kg/m^3 , then the minimum thickness of source cannot be less than 1.48 km (Fig. 7), because the ideal bodies and therefore all solutions confined to smaller thicknesses have densities exceeding 320 kg/m^3 .

The ideal body inversion results helped reduce ambiguity in the interpretation of the gravity anomaly field, and were used as constraints in the 3D modelling process.

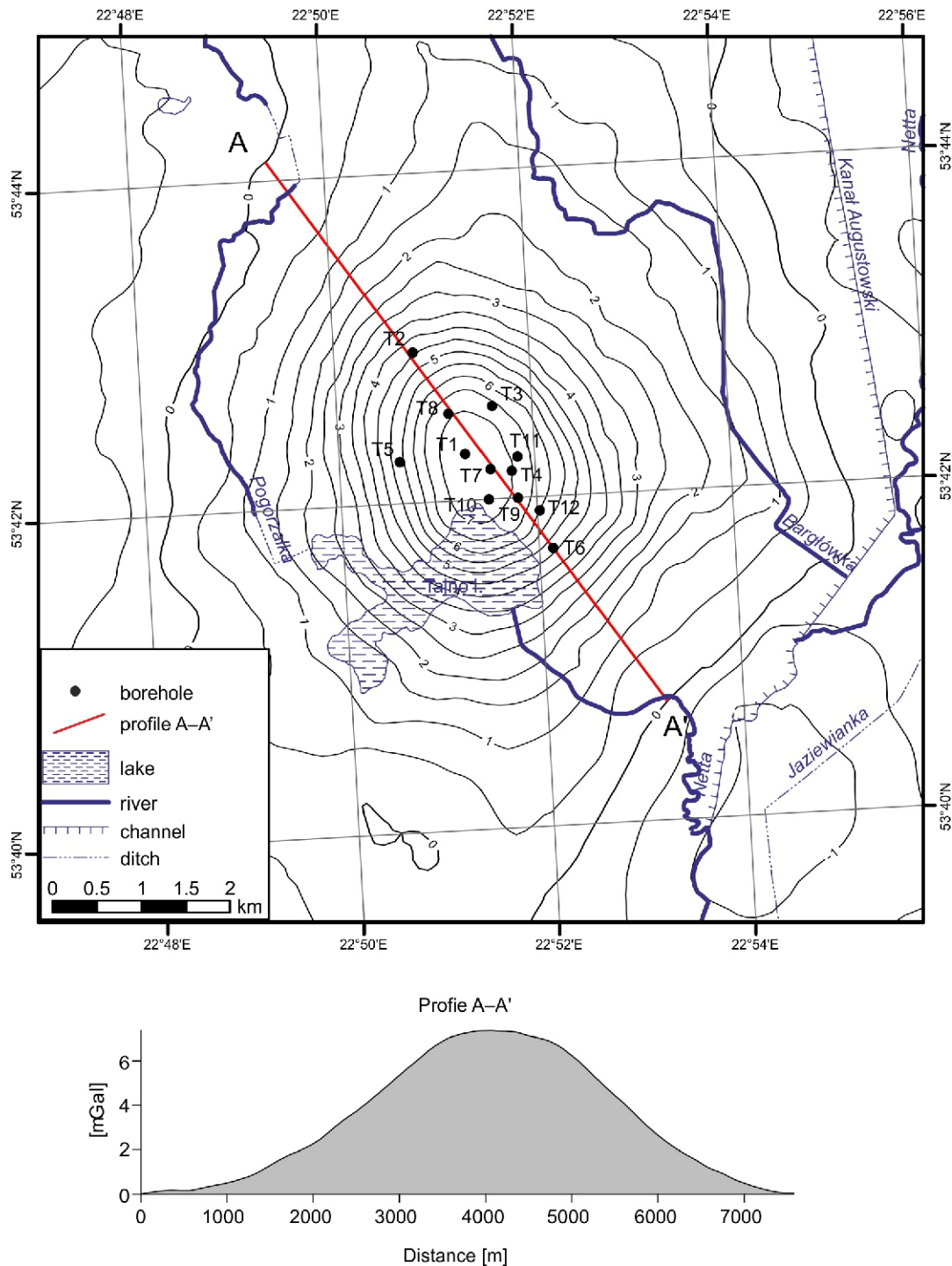


Fig. 6. Residual gravity anomaly map obtained using a high-pass filter with a cut-off wavelength of 20 km applied to the Bouguer gravity anomaly; the gravity data along the A–A' gravity profile were used to calculate ideal body parameters

3D GEOLOGICAL AND GEOPHYSICAL MODELLING OF THE TAJNO MASSIF

The 3D geological model of the Tajno massif was created using *GeoModeller* software (BRGM and Intrepid Geophysics Company) for modelling complex three-dimensional geological structure, taking into account available geological data, namely the geological map, a digital terrain model (DTM), structural data related to the geological boundaries, borehole data, and geological interpretations (Calcagno et al., 2008). This method

has been checked successfully in complex geological conditions (Martelet et al., 2004; Maxelon and Mancktelow, 2005; Putz et al., 2006; Schreiber et al., 2010).

METHODOLOGY

The original method implemented in *GeoModeller* makes use of observations that define the location of interfaces (boundaries) between geological formations, structural observations that provide the orientation of these interfaces, and a

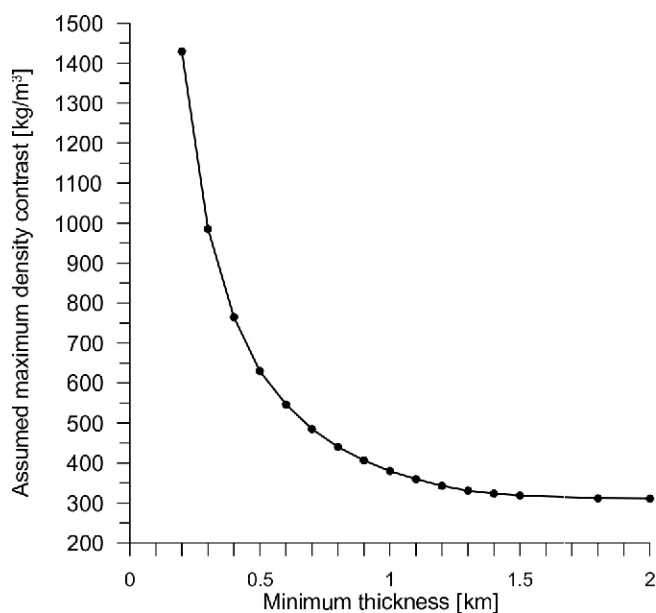


Fig. 7. Trade-off curve for assumed density contrast versus minimum thickness of the causative gravity source, where its top is 0.6 km below the surface, and allowing for up to 0.1 mGal of misfit

Black dots represent calculated minimum density contrasts for a given thickness of the ideal body

geological column (or pile) that shows chronologically ordered geological formations of a region, and the geometrical relationships between particular geological formations. The geological interface is considered as an iso-surface of a scalar potential field which is continuously defined in 3D space, and its dip is represented by the gradient of the potential (Lajaunie et al., 1997). Complex geology, where geological formations cut across or onlap onto each other, is modelled by combining multiple potential field iso-surfaces related to several geological interfaces. A unique solution for the 3D geometry of the interfaces between geological formations that honour all the data is obtained using the cokriging method and geological column which defines the chronological order of the interfaces and the relationships between adjacent geological formations, coded as either “erode” or “onlap”.

Fault relationships can also be defined, allowing complex fault networks and timing relationships between faults and geological formations. A complete description of the 3D *GeoModeller* method is described by Calcagno et al. (2008).

A complementary methodology has been developed to validate a geological model by forward modelling and stochastic inversion of geophysical data, and implemented in *GeoModeller* (Guillen et al., 2008). In this case, the geological model is represented as an assembly of homogeneous volume element (‘voxel’), and the geological model is discretized into a 3D matrix of ‘voxels’, or ‘voxet’. For each ‘voxel’, the appropriate geological formation is assigned. Then, each ‘voxel’ is assigned petrophysical parameters such as density, MS and NRM representative of the geological formation, and the a priori probability density function (in the case of inversion) for each petrophysical parameter and for each geological formation. The computed gravity or magnetic effect of the 3D geological model can be compared to the corresponding measured potential fields.

Given the unknown uncertainties in determining the location of the lithological boundaries and physical property distributions

assigned to each geological formation of the Tajno massif, only forward modelling was performed in this project.

BUILDING THE 3D GEOLOGICAL MODEL

To build a 3D geological model of the Tajno massif, a digital terrain model (DTM), geological data from twelve boreholes, an interpreted subsurface geological map (Fig. 2B) and three cross-sections (Fig. 8), gravity and magnetic data (Fig. 3), and a set of modelling assumptions were used. The model covers an area 10 × 10 km and extends to a depth of 2 km.

The first step of the modelling process is to construct the geological pile for the model. Borehole data have been used to select geological formations to be modelled. The stratigraphy of the sedimentary cover and the lithology of the basement rocks deduced from the boreholes allowed distinction of 15 modelled geological formations (plus 3 unconformities). Two of these are not present in the final model. These are veins of felsic volcanic rock and melanephelinite. Both rock types occurs in small amounts in the geological cross-sections (Fig. 8) – too small to influence the gravimetric or magnetic response of the model. The relationships between each geological formation, i.e. ‘onlap’ or ‘erode’ have been established. All igneous formations have been classified as ‘erode’, and this should not be understood as a classic stratigraphic discontinuity but as a younger rock intruding an older one. The geological relationship has been assigned for the base of each formation to properly map the lower surfaces of the formations. The sequence of the geological formations, chronologically ordered, and their geological relationships (geological pile) for the 3D model of the Tajno massif is shown in Figure 9. Density and magnetic properties were assigned to each of the geological formations of the pile, based on estimates indicated in Table 2. Next, the interpreted boundary of geological formations along geological cross-sections (Fig. 8) and from the map of the crystalline basement (Fig. 2B), were incorporated into the *GeoModeller* software. Geology orientation data were assumed to be orthogonal to the geological boundaries. Three main faults surrounding the whole massif are inserted into model structure. Each of these is present on the geological maps and is interpreted from borehole data.

An initial coherent 3D geological model of the massif based on integration of geological data in the *GeoModeller* software was tested by comparing computed 3D gravity and magnetic effects with maps of measured gravity and magnetic anomalies. The results of the forward gravity and magnetic modelling show spatial differences between the observed and the calculated anomalies. The misfit values of initial model were between –3 and 2.1 mGal for gravity data and between –350 and 420 nT for magnetic data. Such discrepancies suggested that the model geometry or the physical properties of the rocks (and probably both of these) were not correct.

To overcome this problem the geological cross-sections were modified and extra sections were added for the purpose of better model construction. In those cases where the mismatch between observed and calculated anomalies was moderate, the physical properties of the rocks were slightly modified until a better match was obtained. Moreover, it was found that the assumed values of magnetic properties of pyroxenite, hybrid rocks and intrusive breccia (Table 2) were too large to explain the magnetic anomalies observed. In this case, the remanent magnetizations of these rock units were reduced until a better fit was obtained.

Geological and geophysical forward modelling were run in the subsequent iteration mode. After each iteration the com-

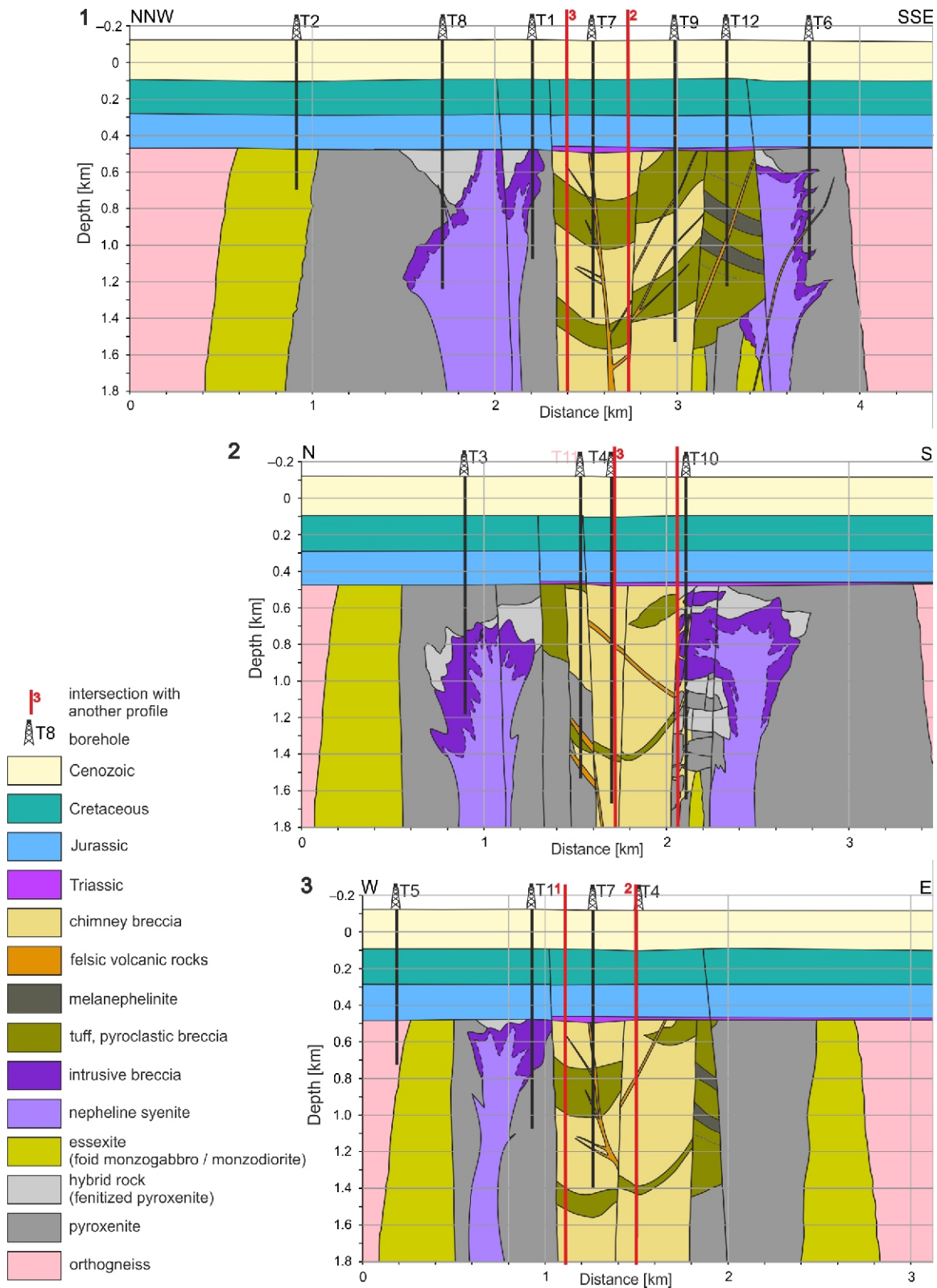


Fig. 8. Geological cross-section 1, 2 and 3 (location Fig. 2B) of the Tajno massif

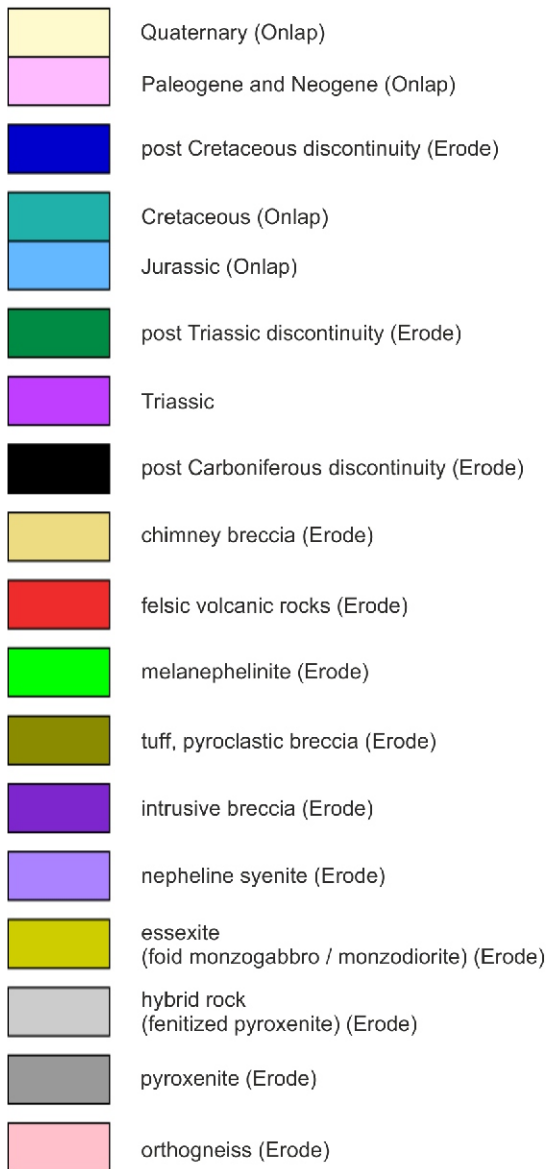


Fig. 9. Geological pile for the Tajno massif area

puted and observed gravity and magnetic anomalies were compared. On the basis of these comparisons revisions were made to the 3D geological model until the resulting model was compatible with observed gravity and magnetic anomalies.

This procedure resulted in considerably improved fits between the final modelled and the observed gravity and magnetic anomalies (Fig. 10). The misfit values were mostly between -0.5 and 0.5 mGal for gravity data (where values of measured Bouguer anomalies vary in the range from 12 to 24 mGal, amplitude: 12 mGal) and between -100 and 100 nT for magnetic data (where values of measured magnetic anomalies vary in the range from -70 to 1860 nT, amplitude 1930 nT), in the spatial zone covering the massif. The final physical properties of the rocks forming the Tajno massif following 3D geophysical modelling are shown in Table 3. The highest discrepancy – excess of rock mass – in the density model appears at the southern and northern peripheries of the modeled block, where no geological constraints (boreholes) exist. The same is true for the north-eastern corner of the magnetic model.

In the centre of the Tajno massif there is a mass deficit in the density model with a good fit to the magnetic model. Some

consensus had to be made in any model, and a better fit of the magnetic model was chosen in this case.

Illustration of the final 3D model of the Tajno massif is shown in Figure 11, and the geological sections through the model (Fig. 12) are along the lines of the original geological sections (Fig. 8). Generally the final model supports the original structure shown in geological cross-sections (Fig. 8) but some significant changes had to be made. A much larger proportion of nepheline syenite displacing pyroxenite appears at the northern and southern parts of cross-sections 1 and 2. At the eastern part of cross-section 3, pyroxenite is partially replaced by tuff and pyroclastic breccia - which results in a wider volcanic chimney. The volcanic chimney is now directly in contact with essexite (foid monzogabbro/monzodiorite). Moreover, such change in the structure causes decrease of the fault dip (compare profile 3 in Figs. 8 and 12).

There is a small but distinct magnetic anomaly to the east of the Tajno massif. There is no geological data describing the source of such an anomaly. In the present model the anomaly was explained by a vertically oriented body of pyroxenite penetrating the surrounding orthogneisses. The body shape is a vertical prism with the top surface at 900 m b.s.l.

DISCUSSION AND CONCLUSIONS

Our research has modelled the spatial structure of the buried alkaline-carbonatite Tajno massif situated in the western part of the East European Craton, in NE Poland (Fig. 1). The Tajno massif is a very promising prospect for REE deposits. In the Tajno massif, the carbonatite rocks occur as REE-bearing veins, cement of the chimney breccia and metasomatites, and are mainly limited to the diatreme (Ryka, 1992). Therefore, establishing the 3D geometry of the whole Tajno massif including the diatreme containing potentially economic accumulations of REE, and precise determination of the diatreme boundary, are of great importance. So far, the diatreme boundary has been determined on the basis of geophysical maps as well as upon analyses of petrological and chemical data (Cieśla and Kosobudzka, 1992; Ryka, 1992; Wiszniewska et al., 2020).

A 3D geological model was built with the 3D *GeoModeller* software which interpolates complex geology using a potential field method. Previously, knowledge of the deep structure of the entire massif was based on a few, unevenly distributed boreholes and one geological cross-section (Kubicki, 1992).

A 3D geological model of the massif was compiled based on limited drilling information and geological and geophysical interpretations. A new geological map of the Tajno massif (Fig. 2B) and three cross-sections (Fig. 8) were drawn based on reinterpretation of borehole, magnetic and gravity data together with the available geological map (Ryka, 1992). At any stage during the model construction, the 3D gravity and magnetic contributions of the model were calculated and compared to the measured geophysical anomalies for further interactive refinement of the model geometry.

Based on the results obtained, the geometry of interfaces in the initial geological model together with physical rock properties - taken as the mean values of values measured on borehole cores – did not solve the problem of some geophysical signatures. It was also found that the proposed distribution of pyroxenites within the massif gave too strong a magnetic response of the model, since pyroxenites are characterized by very high values of magnetic susceptibility and remanent magnetization (Table 1). Therefore the model had to be developed through successive iterations (structure correction – model calculation). Forward gravity and magnetic modelling of the 3D

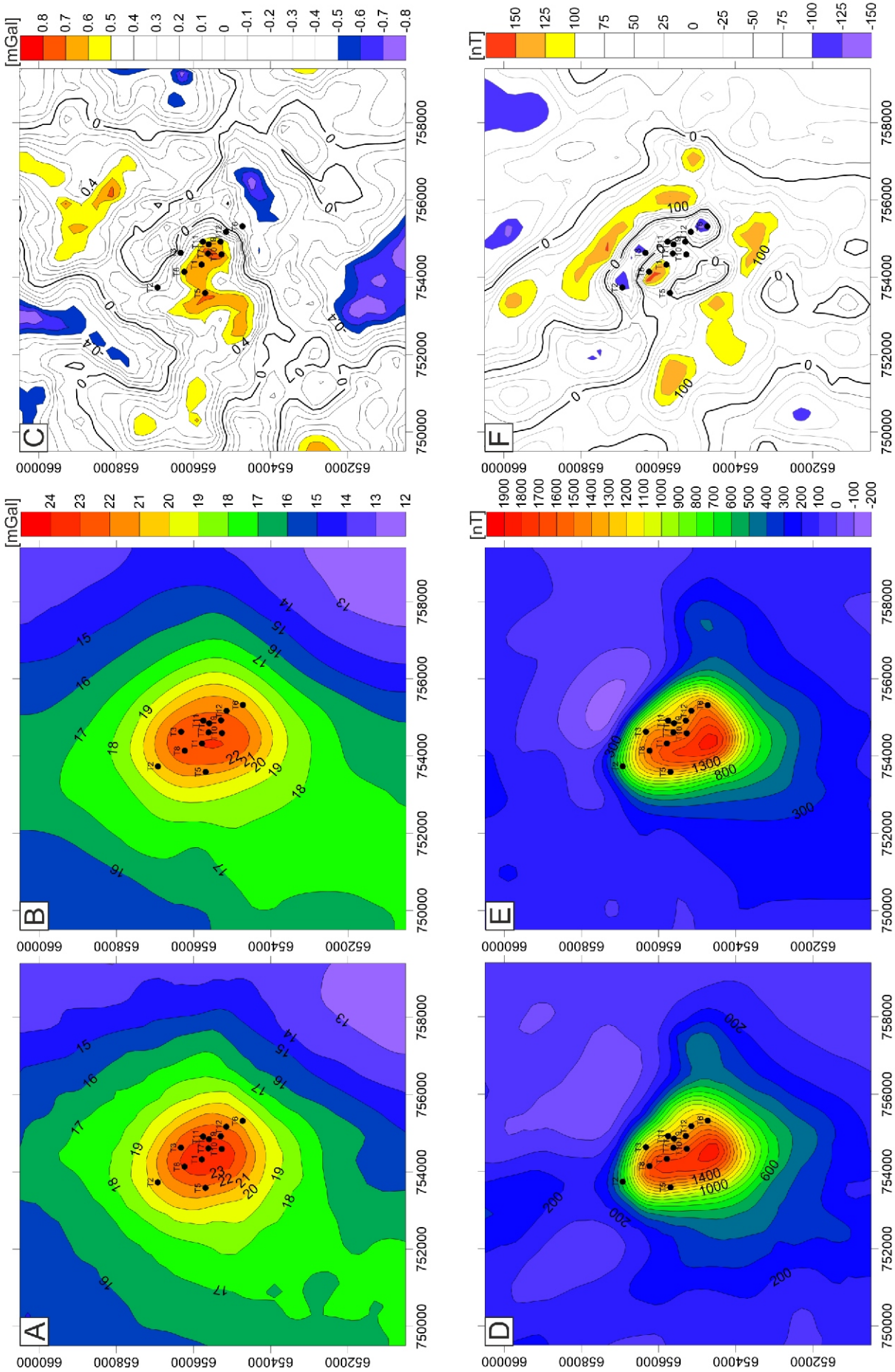


Fig. 10. Comparison between observed and calculated gravity and magnetic anomalies of the final model

A – measured Bouguer gravity anomaly; **B** – calculated gravity response of the final model; **C** – gravity misfit – difference between A and B; **D** – measured magnetic anomaly; **E** – calculated magnetic anomaly; **F** – magnetic misfit – difference between D and E

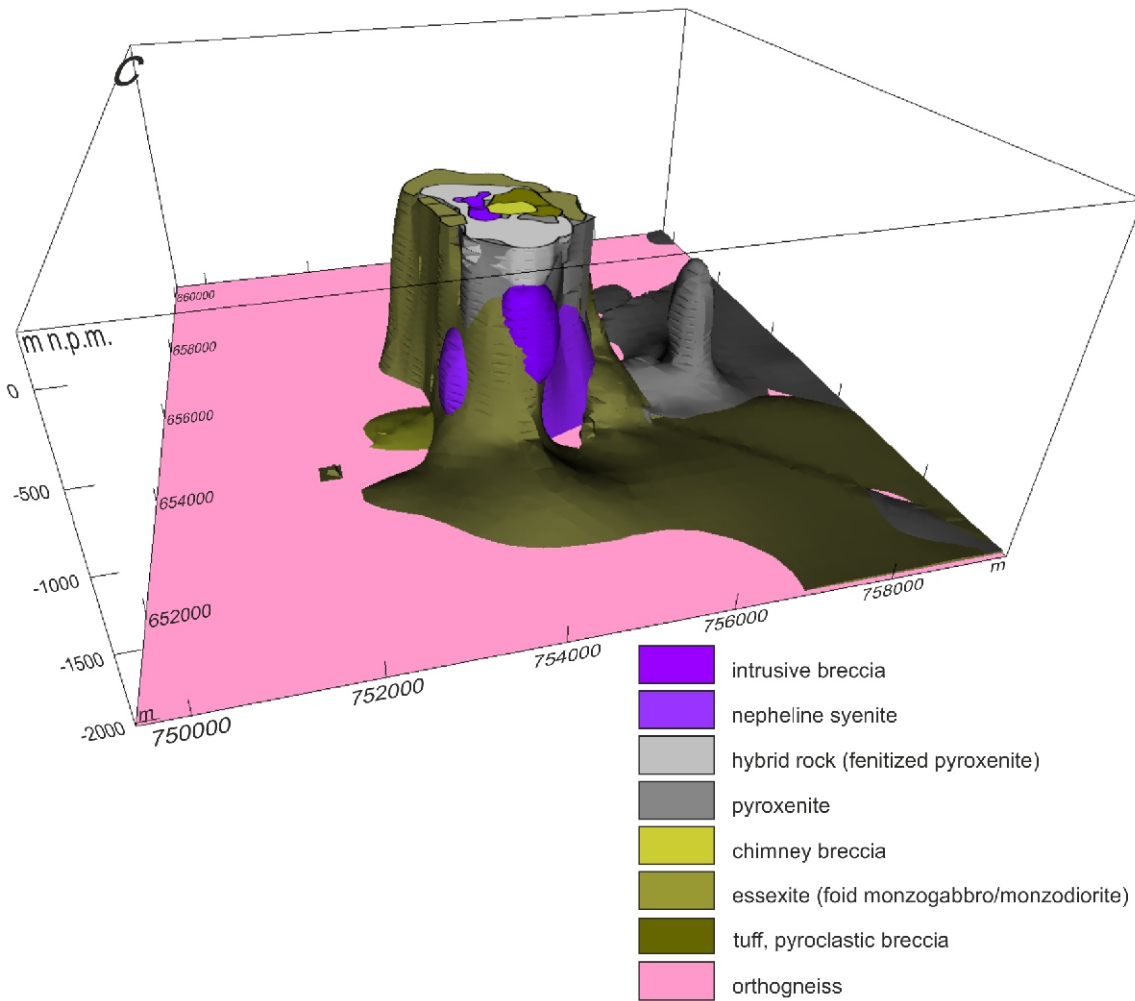


Fig. 11. Perspective view of the final 3D geological model

The colours of the geological units are as shown in [Figure 9](#)

Tajno geological map was carried out, ensuring good agreement between the model architecture, estimates of the physical properties derived from the limited sampling and the observed potential field data.

Modifications to the distributions of pyroxenite, nepheline syenite and intrusive breccia ([Fig. 12](#)) and to the magnetic rock properties of pyroxenite, hybrid rocks and intrusive breccia ([Table 3](#)) in a revised model ([Fig. 11](#)) improved the compatibility with the gravity and magnetic data ([Fig. 10](#)). The comparison between [Figure 10A and B](#) shows a satisfying correlation between the Bouguer anomaly and model gravity effect ([Fig. 10C](#)). The average difference between both grids is 0.0044 mGal and standard deviation is 0.33 mGal. Similarly to the gravity, the result of the forward magnetic modelling again shows different ranges and different spatial arrangements between the observed and the calculated grids ([Fig. 10F](#)) with a mean value of -17 nT and standard deviation of 62 nT.

The main discrepancies are located in the central part of the map ([Fig. 10C](#)) where possible lateral effects of shallow local concentration of higher density material within one of the geological formations might not have been taken into account. However, that geological formations distinguished are commonly a mixture of lithologies with different physical properties, leading to the uncertainty of the physical property data.

The differences between the observed and the calculated grids ([Fig. 10C and F](#)) are not geologically relevant given the uncertainties in determining the location of the boundaries and physical property distributions assigned to each geological formation. A good match between the observed and modelled potential field may be made using the stochastic inversion method implemented in 3D *GeoModeller*. The final result in this type of modelling is strongly dependent on the parameters chosen and constraints applied. Thus, it is very important to use a reference geological model that is consistent with all of the geological ob-

Table 3

Modelled values of the density and magnetic properties of sedimentary rocks and different types of crystalline basement rocks (the values from Table 2 are included in italics)

Geological formation		Density [kg/m ³]	Magnetic susceptibility [SI]	NRM intensity [A/m]	Inclination [°]	Declination [°]
Cenozoic	Quaternary	1700 <i>1700</i>	0 <i>0</i>	0 <i>0</i>	0 <i>0</i>	0 <i>0</i>
	Paleogene and Neogene	1700 <i>1700</i>	0 <i>0</i>	0 <i>0</i>	0 <i>0</i>	0 <i>0</i>
Cretaceous		1750 <i>1750</i>	0 <i>0</i>	0 <i>0</i>	0 <i>0</i>	0 <i>0</i>
Jurassic		1780 <i>1780</i>	0 <i>0</i>	0 <i>0</i>	0 <i>0</i>	0 <i>0</i>
Triassic		2150 <i>2150</i>	0 <i>0</i>	0 <i>0</i>	0 <i>0</i>	0 <i>0</i>
Chimney breccia		2760 <i>2750</i>	0.1 <i>0.02</i>	1.1 <i>1.1</i>	69 <i>21.6</i>	0
Felsic volcanic rocks		2770	0.03	0	0	0
Melanephelinite		2990 <i>2290</i>	0.15 <i>0.15</i>	1 <i>0.2</i>	50 <i>69</i>	0
Tuff, pyroclastic breccia		2870 <i>2850</i>	0.125 <i>0.125</i>	0.9 <i>0.9</i>	40 <i>40</i>	0
Intrusive breccia		2900 <i>2900</i>	0.14 <i>0.14</i>	1.5 <i>15</i>	69 <i>69</i>	0
Nepheline syenite		2660 <i>2660</i>	0.06 <i>0.06</i>	2.0 <i>2.0</i>	69 <i>40</i>	0
Essexite (foid monzogabbro /monzodiorite)		3030 <i>3030</i>	0.18 <i>0.20</i>	3.1 <i>3.93</i>	35 <i>42.3</i>	60
Hybrid rock (fentized pyroxenite)		3170 <i>3170</i>	0.19 <i>0.20</i>	1.66 <i>16.6</i>	69 <i>69</i>	0
Pyroxenite		3320 <i>3300</i>	0.3 <i>0.28</i>	3.1 <i>28</i>	69 <i>69</i>	45
Orthogneiss		2700 <i>2710</i>	0.067 <i>0.05</i>	0.75 <i>0.88</i>	69 <i>30</i>	0

servations, and also closely takes into account the observed geophysical data for most of the study area. As a consequence, the inversion will not provide any significant help to the knowledge of the architecture of the Tajno massif over and above what has already been achieved by forward modeling.

After modifications to the initial model and physical properties, the final model (Figs. 11 and 12) largely confirmed the earlier geological interpretation along three cross-sections (Fig. 11), but a few differences need to be noted:

- a higher proportion of nepheline syenites in relation to pyroxenites;
- a smaller proportion of chimney breccia relative to tuffs and volcanic breccia within the chimney.

The modelling results depend on the quantity and quality of the data used. The main limitation of the model is due to an insufficient number of deep boreholes, so the geology of the massif may be more complex than shown in the current 3D geological model. Another important limitation of the final model results from the wide range of rocks detected and the distribution of magmatic bodies in the massif, which remains poorly constrained. Due to limited amount of geological data, detailed relationships between units are beyond the scope of this work. Nev-

ertheless, the model obtained is the first coherent three-dimensional geological model of the Tajno massif which integrates all geological and geophysical data. On this basis, some important implications of the modelling can be further analysed. For example, the present study makes it possible to constrain the 3D geometry of the carbonatite formations, which we represent basic data for the identification of possible REE reservoirs that may be considered as targets for future prospective drilling. The model can be relatively quickly updated in the future, following the addition of new data or different interpretations of the existing data.

Acknowledgements. Funding of the present work was provided by the Polish Geological Institute-National Research Institute statutory funds (project no. 62.9012.1972.00.0). The authors would like to thank the reviewers: Mateusz Mikołajczak and Mariusz Majdański for their valuable suggestions and constructive comments on the original manuscript. We would also like to thank the Associate Editor Jacek Szczepański for many helpful suggestions and efficient editorial handling, which improved the quality of manuscript.

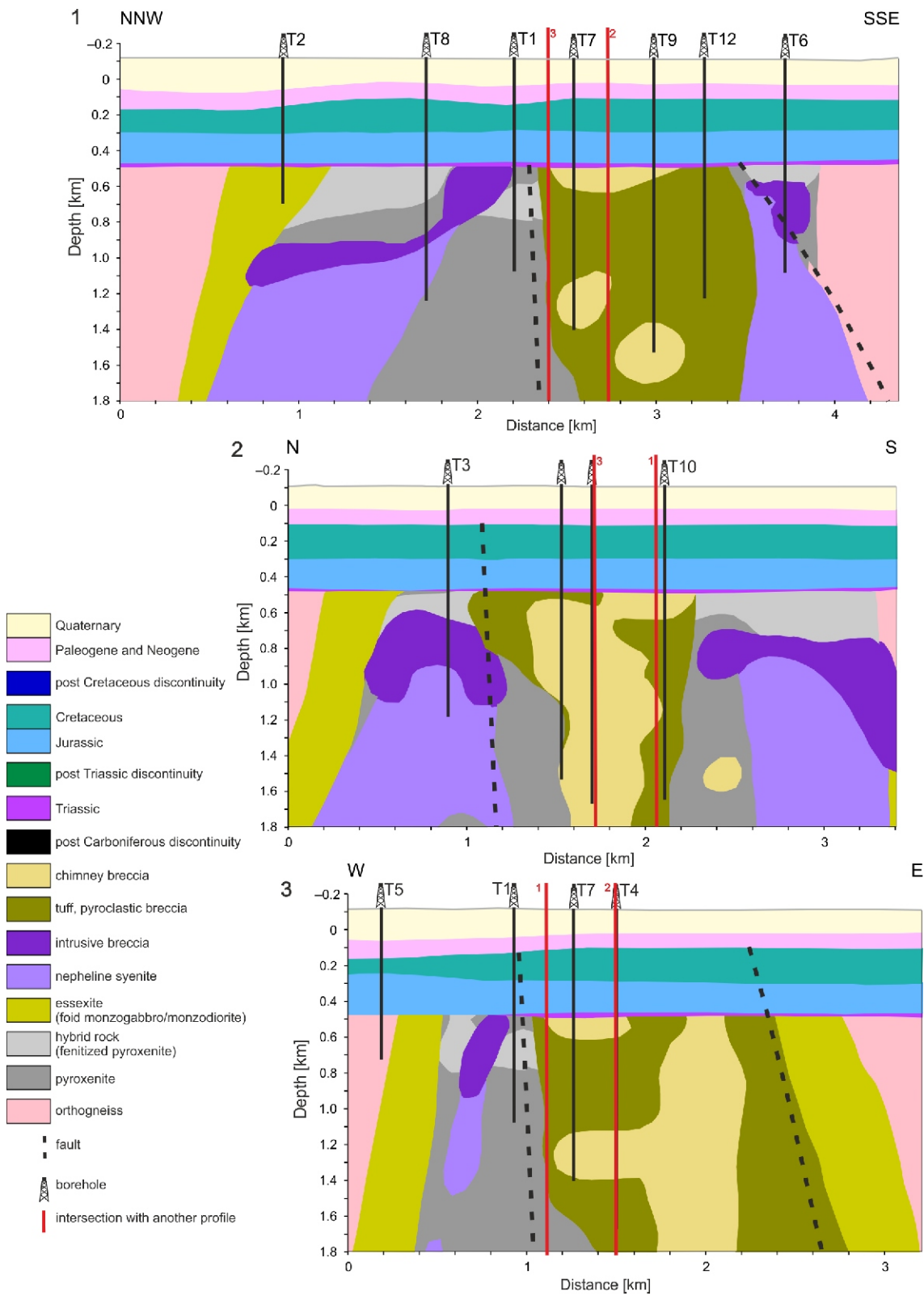


Fig. 12. Modelled geology along sections 1, 2 and 3 (location Fig. 2B) of the Tajno massif

The colours of the geological units are as shown in [Figure 9](#)

REFERENCES

- Blakely, R.J., 1995.** Potential Theory in Gravity and Magnetic Applications. Cambridge University Press, Cambridge.
- Bogdanova, S., Gorbatshev, R., Skridlaite, G., Soesoo, A., Taran, L., Kurlovich, D., 2015.** Trans-Baltic Palaeoproterozoic correlations towards the reconstruction of supercontinent Columbia/Nuna. *Precambrian Research*, **259**: 5–33.
- Calcagno, P., Chiles, J.P., Courrioux, G., Guillen, A., 2008.** Geological modelling from field data and geological knowledge: Part I, Modelling method coupling 3D potential-field interpolation and geological rules. *Physics of the Earth and Planetary Interiors*, **171**: 147–157.
- Cieśla, E., Kosobudzka, I., 1992.** Geophysical studies of the Tajno massif. *Prace Państwowego Instytutu Geologicznego*, **139**: 15–18.
- Demaiffe, D., Wiszniewska, J., Krzemińska, E., Williams, I.S., Stein, H., Brassinnes, S., Ohnenstetter, D., Deloule, E., 2013.** A hidden alkaline and carbonatite province of early Carboniferous age in northeast Poland: zircon U-Pb and pyrrhotite Re-Os geochronology. *The Journal of Geology*, **121**: 91–104.
- Guillen, A., Calcagno, P., Courrioux, G., Joly, A., Ledru, P., 2008.** Geological modelling from field data and geological knowledge, Part II. Modelling validation using gravity and magnetic data inversion. *Physics of the Earth and Planetary Interiors*, **171**: 158–169.
- Huestis, S.P., Ander, E., 1983.** IDB2 - A Fortran program for computing extremal bounds in gravity data interpretation. *Geophysics*, **47**: 999–1010.
- Królikowski, C., Petecki, Z., 1995.** Gravimetric Atlas of Poland. Państwowy Instytut Geologiczny, Warszawa.
- Krystkiewicz, E., Krzemiński, L., 1992.** Petrology of the alkaline-ultrabasic Tajno massif. *Prace Państwowego Instytutu Geologicznego*, **139**: 19–35.
- Krzemińska, E., Krzemiński, L., Petecki, Z., Wiszniewska, J., Salwa, S., Żaba, J., Gaidzik, K., Williams, I.S., Rosowiecka, O., Taran, L., Johansson, L., Pécskay, Z., Demaiffe, D., Grabowski, J., Zieliński, G., 2017.** Geological map of crystalline basement in the Polish part of the East European Platform 1:1 000 000. Państwowy Instytut Geologiczny, Warszawa.
- Kubicki, S., 1992.** An outline of geological structure of the Tajno massif. *Prace Państwowego Instytutu Geologicznego*, **139**: 7–18.
- Kubicki, S., Ryka, W., 1982.** Geological Atlas of Crystalline Basement in Polish Part of the East-European Platform, 1:500 000. Instytut Geologiczny, Warszawa.
- Lajaunie, C., Courrioux, G., Manual, L., 1997.** Foliation fields and 3D cartography in geology: principles of a method based on potential interpolation. *Mathematical Geology*, **29**: 571–584.
- Martelet, G., Calcagno, P., Gumiaux, C., Truffert, C., Bitri, A., Gapais, D., Brun, J.P., 2004.** Integrated 3D geophysical and geological modelling of the Hercynian Suture Zone in the Champtoceaux area (south Brittany, France). *Tectonophysics*, **382**: 117–128.
- Maxelon, M., Mancktelow, N.S., 2005.** Three-dimensional geometry and tectonostratigraphy of the Pennine zone, Central Alps, Switzerland and Northern Italy. *Earth-Science Reviews*, **71**: 171–227.
- Parker, R.L., 1974.** Best bounds on density and depth from gravity data. *Geophysics*, **39**: 644–649.
- Parker, R.L., 1975.** The theory of ideal bodies for gravity interpretation. *Geophysical Journal of the Royal Astronomical Society*, **42**: 315–334.
- Petecki, Z., 2019.** Ideal body analysis of the Pomerania Gravity Low (northern Poland). *Geological Quarterly*, **63** (3): 558–567.
- Petecki, Z., Rosowiecka, O., 2017.** A new magnetic anomaly map of Poland and its contribution to the recognition of crystalline basement rocks. *Geological Quarterly*, **61** (4): 934–945.
- Putz, M., Stuwe, K., Jessell, M., Calcagno, P., 2006.** Three-dimensional model and late stage warping of the Plattengneis Shear Zone in the Eastern Alps. *Tectonophysics*, **21**: 87–103.
- Ryka, W., 1992.** Geology of the Tajno massif carbonatites. *Prace Państwowego Instytutu Geologicznego*, **139**: 43–77.
- Ryka, W., Armbrustmacher, T.J., Modreski, P.J., 1992.** Geochemistry and petrology of the alkaline rocks of the Tajno complex (Preliminary report). *Prace Państwowego Instytutu Geologicznego*, **139**: 37–41.
- Schreiber, D., Jean-Marc Lardeaux, J.-M., Martelet, G., Courrioux, G., Guillen, A., 2010.** 3-D modelling of Alpine Mohos in Southwestern Alps. *Geophys. J. Int.*, **180**: 961–975.
- Wiszniewska, J., Petecki, Z., Krzemińska, E., Grabarczyk, A., Demaiffe, D., 2020.** The Tajno ultramafic-alkaline-carbonatite massif, NE Poland: a review. *Geophysics, petrology, geochronology and isotopic signature. Geological Quarterly*, **64** (2): 402–421.